Cruise Report
RV Poseidon cruise P338

Start: June 2nd 2006 (Piraeus) End: June 13th 2006 (Piraeus)

Chief Scientist: Dr. C. Hübscher Captain: M. Schneider

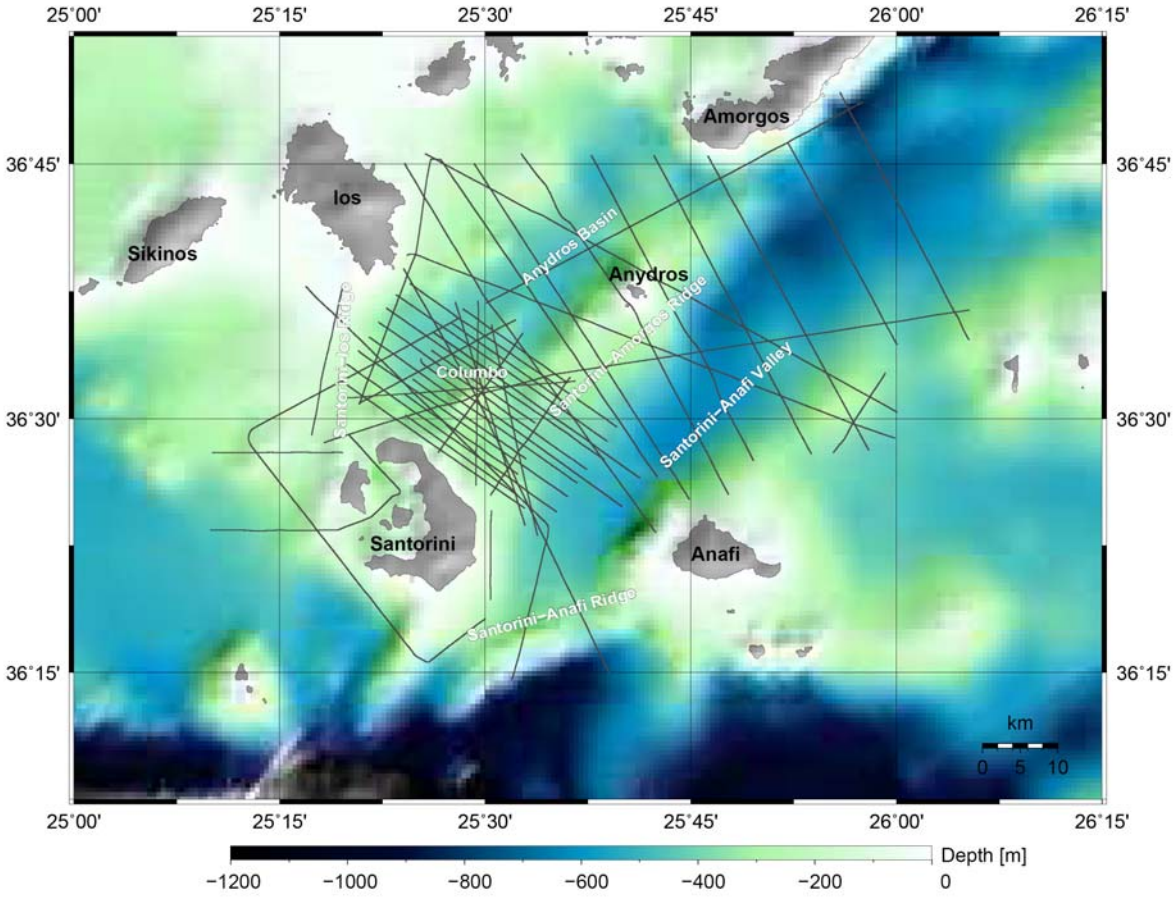

Geophysical profiles surveyed during RV Poseidon cruise P338 (2006)

1. Overview

In the frame of RV Poseidon cruise P338 the Santorini-Amorgos Volcanic Complex has been investigated in spring 2006 by means of profiling geophysical data. More than 1500 km of multichannel seismic and magnetic data as well as 2500 km of gravity data have been collected. The data will allow to reconstruct the Pliocene-Pleistocene tectonic evolution of the investigated area; budgeting of pyroclastic deposits around Santorini and the Coloumbo volcano as well as in the SAZ; and the interpretation of individual eruption events of the Coloumbo and Santorini volcanoes To study the temporal behaviour of volcanic earthquake clusters we installed a network of four Ocean Bottom Seismometers and four Ocean Bottom Tiltmeters on top of the Coloumbo and its vicinity. This experiment further contributed to the international EGELADOS experiment.

2. Participants

Name	Institution (acronym)	Function on board	Nationality
Dr. C. Hübscher	IfG-HH	Chief scientist	German
Dr. G.A. Dehghani	IfG-HH	Scientist	German
M. Beitz	IfG-HH	Scientist	German
M. Hensch	IfG-HH	Scientist	German
B. Hofmann	IfG-HH	Scientist	German
P. Kardas	IfG-HH	Scientist	German
J. Kotkiewicz	IfG-HH	Scientist	German
K. Meier	IfG-HH	Scientist	German
S. Winter	IfG-HH	Technician	German
Prof. Dr. T. Taymaz	ITU	Scientist	Turkish
I. Dimitriadis	DoG	Scientist	Hellenic

IfG-HH: Institute for Geophysics, University of Hamburg
ITU: Istanbul Technical University
DoG: Department of Geology, University of Thessaloniki

3. Scientific Aims

Active tectonic processes along the African-Eurasian collision zone are associated with catastrophic events including earthquakes, major volcanic eruptions, and tsunamis. Understanding how these processes can affect the eastern Mediterranean is of increasing scientific and public interest. The region includes a frequently crossed international sea traffic corridor and dense population centers. Furthermore, most of the small volcanic islands in the Aegean are major tourist attractions that contribute significantly to the wealth of this region.
One of these Aegean islands is Santorini, which is a major explosive volcano and possibly one of the most dangerous volcanoes in Europe. During the past 150 million years, Santorini has had 12 major eruptions, and several of them ejected large columns

of ash and debris high into the atmosphere. It is widely believed that the eruption of Santorini about 3600 years before present (B.P.) destroyed the Minoan civilization of Crete. In addition to the volcanic island, there are several submarine volcanic seamounts in the Aegean Sea. One of them, the Coloumbo seamount, is about eight kilometers northeast of Santorini, and recently has attracted attention due to the high earthquake activity of the Hellenic subduction zone. This activity is concentrated in an area northeast of Santorini, within the so-called Santorini-Amorgos zone.
According to previous findings, the Santorini-Amorgos zone (SAZ) marks a major structural boundary in a dextral transtensional regime that subdivides the Hellenic volcanic arc into a seismically and volcanically quiet western and an active eastern part. The highest earthquake activity has been observed beneath the submarine Coloumbo volcano and northeast of it along the Santorini-Amorgos Ridge, which terminates south of the island of Amorgos.
The activity close to the Coloumbo seamount is considered to be linked directly to a magma reservoir and to be influenced by the migration of magma and fluids toward the surface. Earthquakes northeast of the volcano also may result from magma and associated fluid migration toward the surface, according to some suggestions. The Santorini-Coloumbo volcanic complex includes one caldera at Santorini and one crater at Coloumbo. The caldera of Santorini is formed by four deep basins (from 290 to 390 meters deep). The Coloumbo volcano has a well-defined crater with a single basin (depth 500 meters). Until now, only a single underwater eruption has been reported for the Coloumbo volcano in 1650 A.D.

The general scientific objectives of the first phase of the “Inspecting Coloumbo” project included the investigation of shallow expressions of deep-rooted tectonic or magmatic intrusions, which may result in active faulting or fluid migration, respectively. During the research cruise, the Santorini-Coloumbo complex as well as the SAZ were mapped in detail by means of multichannel seismic reflection and magnetic (1500 kilometers each) and gravity (2500 kilometers) profiling. For the active seismics, a bubble free airgun with about 100-hertz main frequency served as the seismic source. In the sediment basins, the signal penetrated to a depth of more than one kilometer beneath the seafloor. Data were received by two seismic sensor cables (streamers) of 600- and 150-meter length, respectively.
The seismic data will help with (1) the reconstruction of Pliocene-Pleistocene tectonics; (2) the budgeting of pyroclastic deposits around Santorini and the Coloumbo volcano as well as in the SAZ; (3) the interpretation of individual eruption events of the Coloumbo and Santorini volcanoes; and (4) the detection of fluid migration paths and reservoirs associated with magmatic intrusions. The gravity and magnetic data will help to correlate shallow tectonic signals with deeper magmatic intrusions, and therefore determine the distinction between main faults above an intrusion or side branches.

4. Instruments, Profiles and Stations
4.1 Reflection Seismics

The building blocks of the multichannel seismic equipment consist of 1) a seismic sources including an airgun control and trigger system for signal generation and detection, 2) a streamer for signal detection and 3) a seismograph for data recording.

A single G.I. Gun has been used in True G.I. Mode (Injector volume: 45 in3, Generator volume: 105 in3) as seismic source, producing a signal of 100 Hz main frequency. It was towed at a depth of 2.5 m and in a distance of 20 m toward the ship's stern. The gun has been triggered at constant time intervals of 10 s. Assuming an average ship's speed of 5 kn (approximately 2.5 m/s) this results in a shot distance of 25 m. The SureShot trigger system is a modular system of components that can be adapted to the need of 4 Prakla airguns or 2 GI-Guns. The PC based control unit includes a real time card for internal cycle times.
Two different streamers were simultaneously deployed during the measurements. The high resolution streamer of the University of Hamburg consists of a 120 m of tow-lead, two 10 m passive stretch sections, and three 50 active sections. Each active section houses 8 hydrophone groups of 4.9 m length. The distance between groups is 6.25 m, and the number of hydrophones per group is 16. During operation the 1st active group started 40 to 70 m behind the ship‘s stern. The second streamer was a 24 channel streamer with 600m active length giving a group spacing of 25 m. A 200 m stretch gave the necessary initial offset.
The R48 StrataView seismograph is a PC based A/D converter with pre-amplification and anti-alias filtering options. The dynamic range depends on sample rate, but it is always higher than 110 db. The StrataView is connected to the CHAMP (s.a.) and to the CNT-1 controller PC, which performs storing, quality control (QC), and online plotting on the connected laser printer. Demultiplexed data were stored on two daisy chained DAT drives. For security reasons the tape capacity was decreased to 2 Gbyte. Quality control capabilities include several data display windows, which are shot window, gather plot, trigger window, noise window, and tape window. We generally choose a sample rate of 1 ms.
This custom designed charge amplifier matches the impedance between streamer and deck cable on one side and the StrataView seismograph on the other side. The bandpass filter effect of mis-matched impedances can be decreased. Additionally the CHAMP performs signal amplification to enhance the dynamic range.

4.2 Gravity Meter System

During the cruise, the high performance Gravity Meter System KSS30/31 was deployed. The system belongs to the Institute of Geophysics, University of Hamburg and is applied to prospecting and geophysical exploration of the Earth.
The system is organized into three major subsystems including:

- GSS 30 gravity sensor subsystem
- KT 30 stabilisation subsystem
- Data handling subsystem

The gravity sensor subsystem includes a non-astatized springmass assembly as basic gravity detector and control electronics, GE 30, with a voltage pulse rate converter output to the data handling subsystem. The sensor includes a sealed buffered battery unit as power-supply with sufficient capacity to maintain the sensor thermostat for 24 hours in case of a main power failure. Further more, the sensor has its own caging electronics, which activates the sensor caging mechanics in case of failure.

The stabilization subsystem consists of the platform and a vertical electrically erected gyro with two axes. The platform compensates the gravity sensor for roll and pitch. All logic functions of the gyro as well as the automatic platform caging are performed by the system controller ZE30.
The data handling subsystem provides all equipment necessary for filtering, logging, pre-processing and self-testing of gravity measurements. It also provides the control electronics of the platform, the power supply for the sensor, platform and monitor registration facilities.
The central part of data handling system is the system controller ZE 30 consisting of a central processor and the interface to the peripheral equipment such as gyro, platform, gravity meter, externally provided navigation data and the computer for the data logging and processing.
The measuring system, based on a vertical sensor, consists of a tube-shaped mass (30 g) guided by 5 threads in a frictionless manner.
The sensor is non-astatized and the motion of the sensor mass is limited to one degree of freedom in the vertical direction. The constant gravitational acceleration is compensated by a mechanical spring and the gravity changes are detected by an electromagnetic system. The measuring system is housed in the thermostatized, pressure-tight and magnetically shielded section. An optimal tensioning is very important with respect to system sensitivity to external perturbing accelerations. The sensor operates as a zero method system. The mass is always fed back to zero position. The zero position detector is able to detect a mass displacement of less than 10 Å (less than 0.02 mGal).

Accuracy on profile

Vertical Acceleration (mGal RMS)	Sea State	Dynamic * (mGal RMS)	Effective** (mGal RMS)
Less than 15000	Calm sea	0.5	0.2
15000 to 80000	Rough sea	1	0.4
80000 to 200000	Very rough sea	2	0.8

Accuracy during turn maneuver

Vertical Acceleration (mGal RMS)	Sea State	Dynamic * (mGal RMS)	Effective** (mGal RMS)
15000 to 80000	Turn maneuver	2.5***	1***

* Accuracy without applying data reduction.
** Accuracy applying data reduction procedures.
*** Depending on accuracy of navigation data.

The sensor has a built-in scale factor and test facility which can be used in harbour before the cruise starts. The principle consists of putting an additional weight (3 g) to the sensor mass. The additional mass is a ball approximately 2 mm diameter. It is located in the caging device. From a neutral position the ball is displaced by means of a lever and added to the measuring system. The additional mass produces approximately 1000

mGal change in gravity. With this device one can check the measuring system in harbour before the cruise starts.
The interface of ZE 30 to the navigation computer is performed with a standardized serial interface circuitry of RS 232c. The ZE 30 expects the following unfiltered raw data from the navigation computer updated every second in the special format:

- Date and time
- Latitude and Longitude
- Heading and Course
- Speed and Velocity
- Depth

4.3 Gradiometer (Magnetometer)

During the cruise the total intensity of the magnetic field of the earth was recorded along some gravity profiles. The magnetic measurements were carried out using a proton precession Gradiometer type GEOMETRICS G801G (a Gradiometer is a Magnetometer with two sensors). The difference between a Magnetometer and a Gradiometer is that the magnetic measurements with a Gradiometer have no influence of the daily variations of the magnetic Field of the earth where as the measurements of magnetic with a “one sensor magnetometer” included these variations. In order to be able to reduce the measured values of a Magnetometer one need to have a magnetic base station in the area or at least use the recorded magnetic field of an observatory near the research area.
The two sensors of Gradiometer were always towed 250 meters behind the ship with a distance of 10 meters between the two sensors. Although this distance of the sensors from the ship was under the recommended given distance the quality of data recorded was good enough.
The magnetic data were recorded on profiles along the gravity and seismic lines. The data were recorded digitally as well as analogue and were merged with the recorded navigation data. We used the International Geomagnetic Reference Field as the regional field in order to calculate the magnetic rest field.

4.4 Ocean Bottom Seismometer (OBS) and Ocean Bottom Tiltmeter (OBT)

To study the temporal behaviour of volcanic earthquake clusters we installed a network of four Ocean Bottom Seismometers (OBS50-53) and four Ocean Bottom Tiltmeters (OBT54-57) on top of the Coloumbo and its vicinity. This experiment further contributed to the EGELADOS experiment. The OBS-stations were equipped with force balanced broadband seismometers manufactured by PMD. 2 component *Lippmann* tiltmeters have been installed on the OBT. All stations were equipped with hydrophones in order to measure seismic signals. Differential Pressure Gauges to measure long period relative pressure signals from 60 s up to 5 Hz were mounted on OBS 50 and 51.

Instrument	Northing	Easting	Water Depth
OBS50	36°30.00'N	25°27.35'E	287m
OBS51	36°33.18'N	25°31.22E	203m
OBS52	36°30.00'N	25°39.00'E	367m
OBS53	36°38.50'N	25°30.00'E	401m
OBT54	36°31.40'N	25°27.60'E	251m
OBT55	36°31.20'N	25°28.00'E	124m
OBT56	36°30.75'N	25°28.73'E	106m
OBT57	36°30.30'N	25°30.00'E	293m

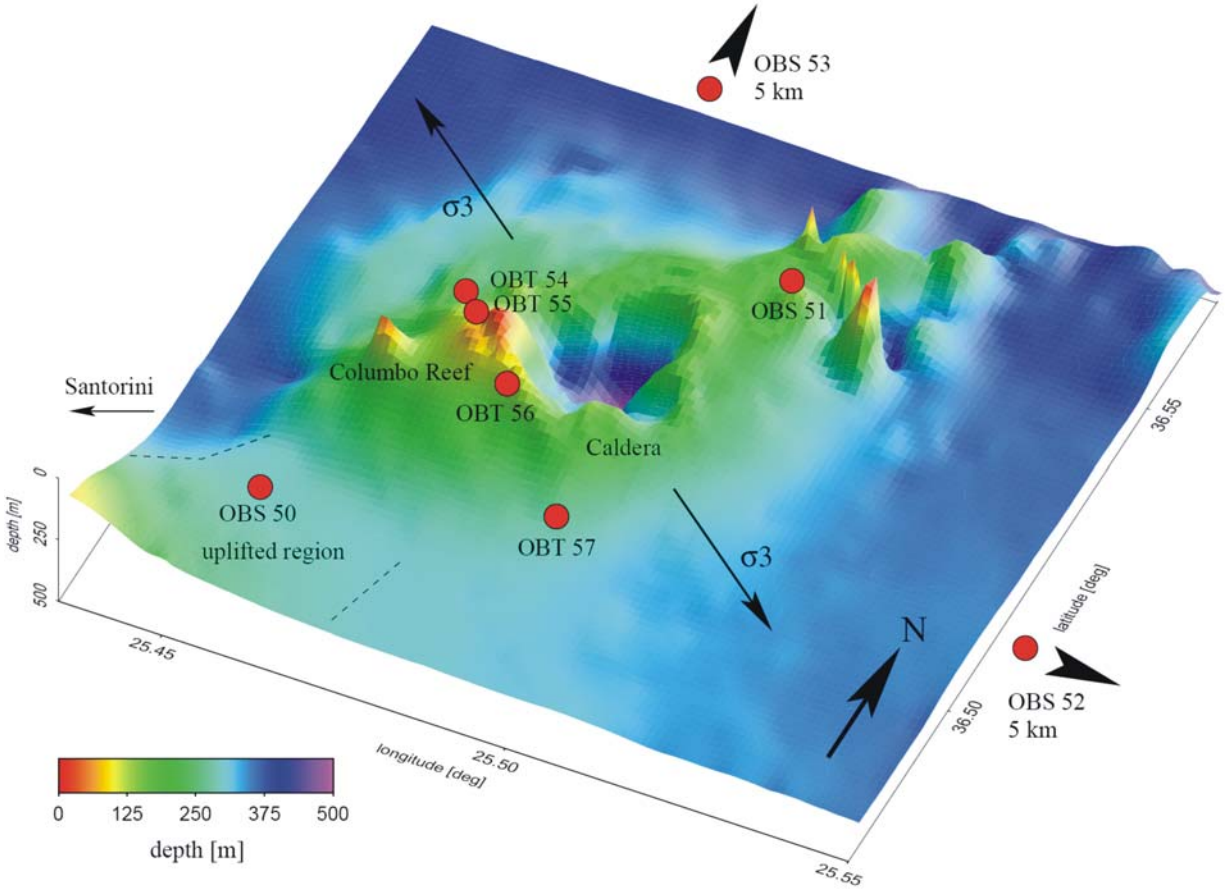

Map showing OBS and OBT locations on Coloumbo seamount.

5. First Results

Seismic cross-sections of the Santorini-Amorgos Ridge where the earthquake activity is highest, indicates that its sediment cover is highly and actively faulted. The presence of magnetic anomalies at the ridge's southeastern escarpment suggests that the earthquake activity and the active faulting are caused by magmatic processes. Initial modeling results suggest that the magnetic source body, such as a magma chamber, lies at a depth of five kilometers. This is consistent with previously published epicenter depths of a few kilometers.

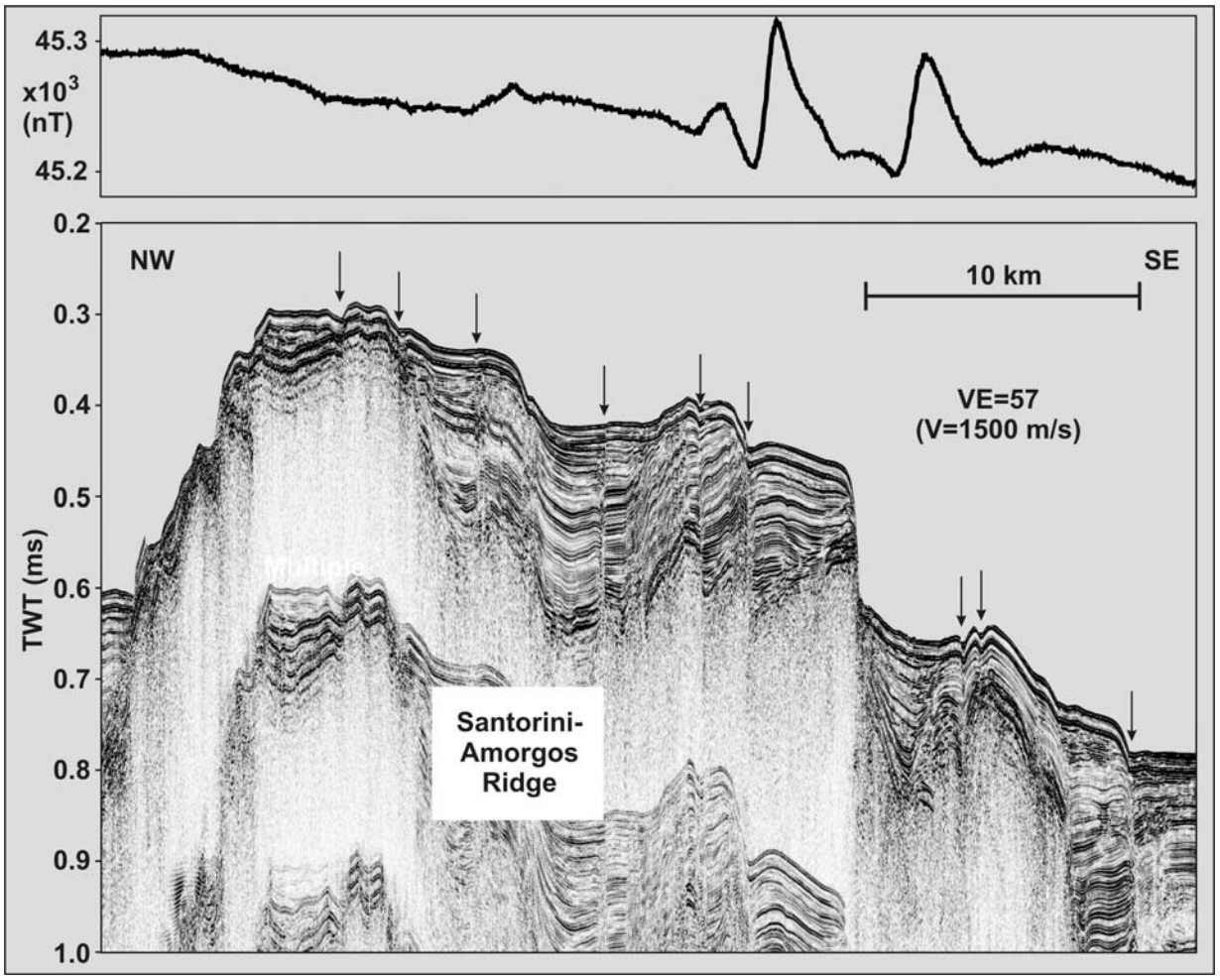

Seismic lines across the Coloumbo volcano elucidate the primary building blocks of the volcano. Two cone-like volcanoclastic deposits show that the Coloumbo volcano evolved from at least two eruptions. A bright spot about 200 meters beneath the caldera provides evidence for gassy and/or fluid charged sediments. The strong magnetic anomaly (~450 nano-teslas) above the caldera can be assumed to be caused by a magma chamber beneath the caldera. In addition, a depth for the magnetic body has been estimated at five kilometers. Southeast of the volcano, along the so-called Kameni line, an elongated

dike intrusion, named the Poseidon Ridge, has been discovered about 100 meters beneath the seafloor. The ridge, six kilometers wide and more than 10 kilometers long, is characterized by a small magnetic anomaly of about 40 nano-teslas. An active extensional fault can be seen on the seafloor. A second extensional fault lineament is present northwest of Coloumbo, where initial faults already pierce the seafloor. Both of these examples prove that the Santorini-Amorgos zone is tectonically active and deserves constant monitoring.

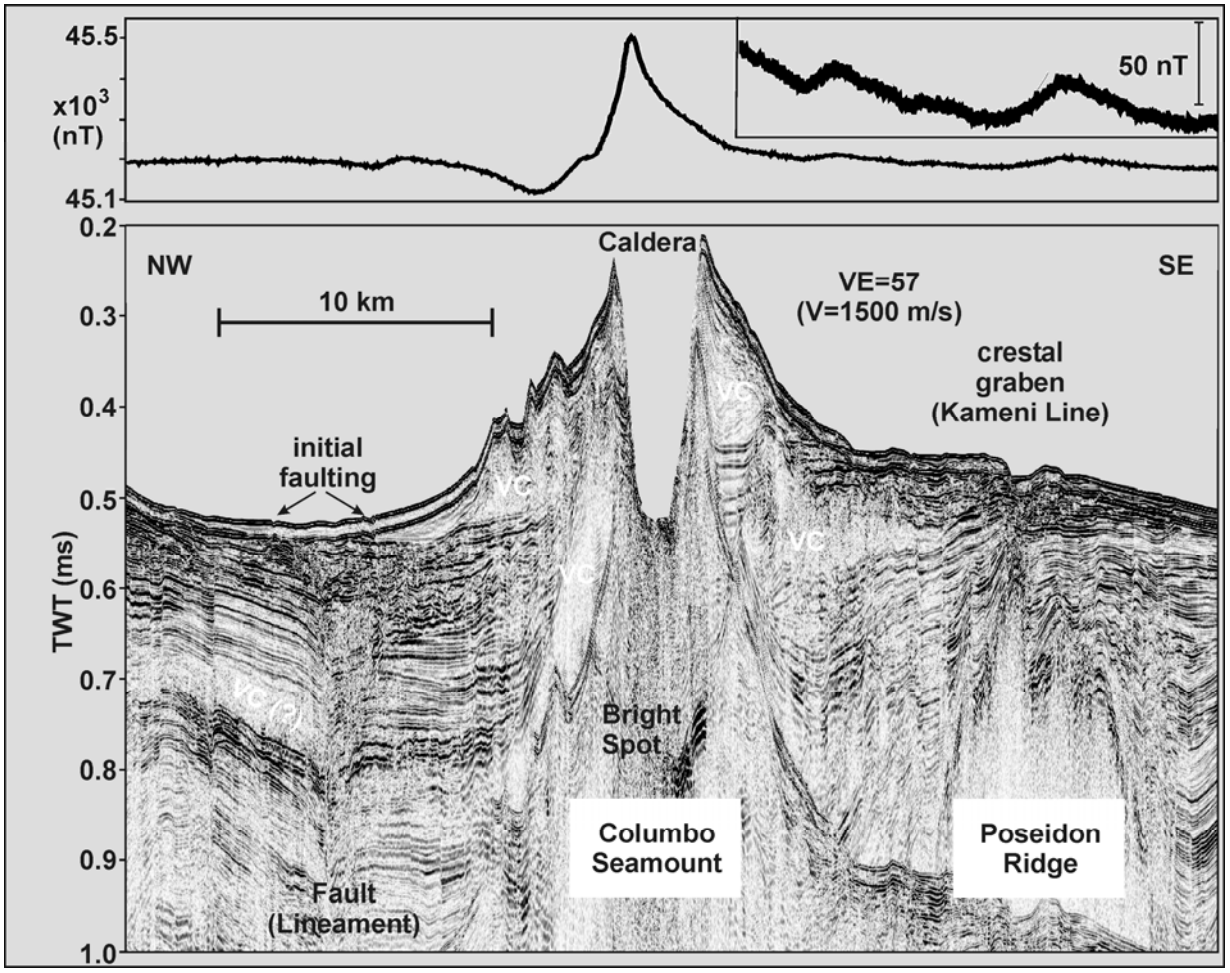

Related publication: Hübscher, C., Hensch, M., Dahm, T., Dehghani, A., Dimitriadis, I., Hort, M., Taymaz, T., 2006. Towards a risk assessment of central Aegean volcanos. EOS 87(39), 401-407.

Acknowledgements

We have to thank Captain M. Schneider and his crew for their outstanding support throughout the entire survey. Cruise P338 and the related research project was funded by the Deutsche Forschungsgemeinschaft DFG. It has been designed in collaboration with the EGELADOS project, a large-scale amphibian deployment of seismic broadband stations all over the Southern Aegean and Western Turkey led by scientists from Ruhr-University Bochum, Germany, in close cooperation with Greek and Turkish scientists.

Appendix: High-resolution profile map and profile list

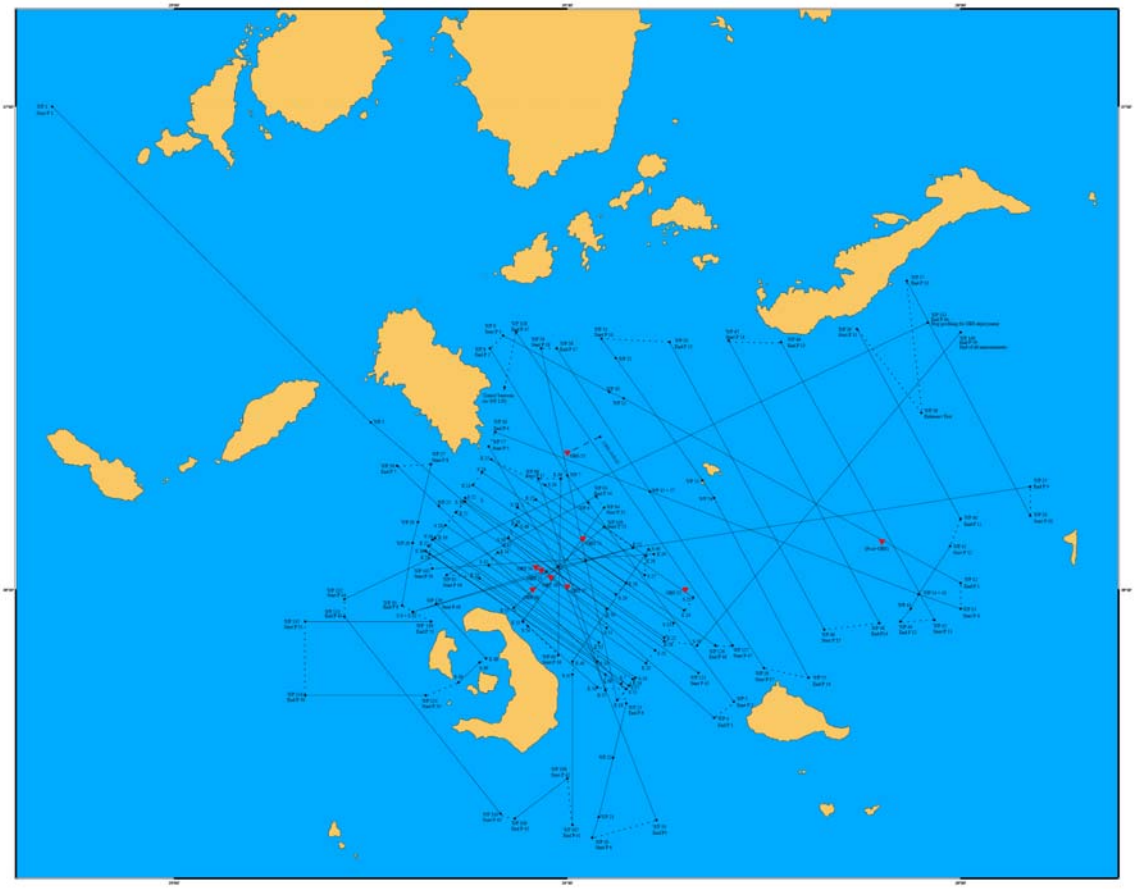

Way Point	Latitude (N)	Longitude (E)	Remark
1	37°00,0'	024°50,7'	Start P1
	36°51,23'	025°01,54'	
	36°44,58'	025°10,70'	
2	36°50,4'	025°15,0'	
3	36°31,1'	025°28,4'	Columbus Seamount
4	36°22,0'	025°41,2'	End P1
5	36°23,0'	025°42,7'	Start P2
6	36°35,4'	025°31,6'	Seamount
7	36°37,1'	025°30,0'	Course change
8	36°45,0'	025°24,1'	End P2
9	36°45,8'	025°25,1'	Start P3
10	36°42,3'	025°33,2'	Seamount
11	36°41,9'	025°34,3'	Seamount
12	36°30,4'	026°00,0'	End P3
13	36°28,8'	026°00,0'	Start P4
14	36°29,7'	025°56,8'	Seamount
15	36°36,1'	025°36,3'	Seamount
16	36°39,8'	025°24,5'	End P4
17	36°38,9'	025°24,0'	Start P5
18	36°31,4	025°29,28'	Columbus Seamount (korr.)
19	36°15,6'	025°36,8'	End P5
20	36°14,5'	025°31,9'	Start P6
21	36°15,8'	025°32,4'	Seamount
22	36°19,5'	025°33,5'	Seamount
23	36°22,9'	025°34,5'	End P6
24	36°24,1'	025°34,1'	Start P7
25	36°35,2'	025°20,2'	Seamount
26	36°37,7'	025°17,0'	End P7
27	36°37,8'	025°19,6'	Start P8
28	36°34,2'	025°18,6'	Seamount
29	36°32,9'	025°18,2'	Seamount
30	36°29,0'	025°17,4'	End P8
31	36°28,6'	025°18,2'	Start P9
31a	36°30,7'	025°26,6'	
31b	36°31,0'	025°28,4'	Seamount
32	36°31,40'	025°29,28'	Columbus Seamount
33	36°31,8'	025°31,4'	Seamount
34	36°32,6'	025°35,0'	Course change

35	36°36,4’	026°05,3’	End P9
36	36°34,6’	026°05,3’	Start P10
37	36°49,2’	025°55,9’	End P10
38	36°41,0’	025°57,0’	Releaser Test
39	36°46,2’	025°52,1’	Start P11
40	36°34,4’	026°00,0’	End P11
41	36°32,7’	025°59,2’	Start P12
42	36°29,7’	025°56,8’	Seamount
43	36°28,8’	025°56,2’	Seamount
44	36°28,0’	025°55,4’	End P12
45	36°28,1’	025°58,0’	Start P13
46	36°45,4’	025°46,3’	End P13
47	36°45,5’	025°42,3’	Start P14
48	36°27,9’	025°53,8’	End P14
49	36°27,5’	025°49,6’	Start P15
50	36°45,4’	025°37,8’	End P15
51	36°45,6’	025°32,6’	Start P16
52	36°44,4’	025°33,7’	Seamount
53	36°36,8’	025°40,3’	Seamount Anydros
54	36°35,7’	025°41,2’	Course change
55	36°24,5’	025°48,4’	End P16
56	36°25,1’	025°45,0’	Start P17
57	36°36,1’	025°36,3’	Seamount = WP15
58	36°45,0’	025°29,2’	End P17
59	36°45,0’	025°28,0’	Start P18
60	36°31,8’	025°31,4’	Seamount = WP33
61	36°23,1’	025°33,8’	End P18
62	36°24,5’	025°35,2’	Start P19
63	36°33,2’	025°19,9’	End P19
64	36°34,0’	025°20,7’	Start P20
65	36°25,4’	025°36,0’	End P20
66	36°26,2’	025°36,7’	Start P21
67	36°34,8’	025°21,5’	End P21
68	36°35,7’	025°22,2’	Start P22
69	36°27,0’	025°37,4’	End P22
70	36°27,9’	025°38,1’	Start P23
71	36°36,5’	025°22,8’	End P23
72	36°37,3’	025°23,5’	Start P24
73	36°28,7’	025°38,9’	End P24
74	36°29,5’	025°39,6’	Start P25
75	36°38,1’	025°24,2’	End P25
76	36°36,5’	025°28,3’	Start P26
77	36°32,1’	025°36,0’	End P26
78	36°30,9’	025°35,9’	Start P27
79	36°35,6’	025°27,6’	End P27
80	36°35,1’	025°26,2’	Start P28
81	36°30,4’	025°34,5’	End P28
82	36°29,7’	025°33,7’	Start P29
83	36°34,0’	025°26,1’	End P29

84	36°33,2’	025°25,5’	Start P30
85	36°28,8’	025°33,0’	End P30
86	36°27,6’	025°33,0’	Start P31
87	36°32,3’	025°24,7’	End P31
88	36°31,5’	025°24,0’	Start P32
89	36°26,7’	025°32,4’	End P32
90	36°25,5’	025°32,3’	Start P33
91	36°30,7’	025°23,3’	End P33
92	36°30,9’	025°20,8’	Start P34
93	36°35,8’	025°32,2’	End P34
94	36°35,1’	025°32,8’	Start P35
95	36°28,0’	025°26,6’	End P35
96	36°25,9’	025°29,3’	Start P36
97	36°36,9’	025°29,5’	End P36
98	36°36,9’	025°27,8’	Start P37
99	36°23,7’	025°32,9’	End P37
100	36°24,7’	025°32,9’	Start P38
101	36°32,2’	025°19,5’	End P38
102	36°31,2’	025°19,7’	Start P39
103	36°32,2’	025°36,6’	End P39
104	36°32,5’	025°36,2’	Start P40
105	36°25,5’	025°30,4’	End P40
106	36°24,7’	025°30,4’	Start P41
107	36°15,3’	025°30,4’	End P41
108	36°18,2’	025°30,0’	Start P42
109	36°15,7’	025°26,0’	End P42
110	36°16,0’	025°24,9’	Start P43
111	36°28,3’	025°13,0’	End P43
112	36°29,4’	025°13,0’	Start P44
113	36°48,6’	025°57,5’	End P44
114	36°33,0’	025°54,0’	OBS 49 (Bochum)
			Poseidons Rock
115	36°39,5’	025°32,5’	OBS 53
116	36°30,0’	025°39,0’	OBS 52
117	36°30,0’	025°27,4’	OBS 50
118	36°33,2’	025°31,2’	OBS 51
119	36°31,4’	025°27,6’	OBT 54
120	36°31,2’	025°28,0’	OBT 55
121	36°30,8’	025°28,7’	OBT 56
122	36°30,2’	025°30,0’	OBT 57
123	36°24,8’	025°40,0’	Start P45
124	36°33,2’	025°25,5’	End P45
125	36°35,1’	025°26,2’	Start P46
126	36°26,5’	025°41,3’	End P46
127/15	36°26,5’	025°42,6’	Start P47
128/16	36°46,0’	025°26,1’	End P47 / Start Transitprofil
129/17	36°29,1’	025°20,0’	Start P48

130/18	36°25,7’	025°23,8’	End P48
131/19	36°25,45’	025°23,3’	Start P49
132/20	36°24,2’	025°21,7’	End P49
133/21	36°23,4’	025°19,2’	End 49 / Start P50
134/22	36°23,4’	025°10,0’	End P50
135/23	36°28,0’	025°10,0’	Start P51
136/24	36°28,0’	025°19,6’	End P51
137/25	36°28,6’	025°18,2’	Start P52
138/26	36°32,6’	025°35,0’	End P52
139/27	36°33,9’	025°32,8’	Start P53

140/28	36°31,44’	025°29,28’	Seamount
141/29	36°28,85’	025°25,9’	End P53
142/30	36°27,7’	025°27,0’	Start P54
143/31	36°23,9’	025°32,3’	End P54
144/32	36°23,8’	025°34,5’	Start P55
145/33	36°32,4’	025°19,2’	End P55
146/34	36°33,1’	025°19,7’	Start P56
147/35	36°24,4’	025°35,0’	End P56
148/36	36°26,5’	025°39,9’	Start P57
149/37	36°46,0’	026°00,0’	End P57